

Research Article

Shell Thickness-Dependent Strain Distributions of Confined Au/Ag and Ag/Au Core-Shell Nanoparticles

Feng Liu,¹ Honghua Huang,² Ying Zhang,² Ting Yu,² Cailei Yuan,² and Shuangli Ye^{1,3}

¹Institute of Microelectronics and Information Technology, Wuhan University, Wuhan, Hubei 430072, China

²Laboratory of Nanomaterials and Sensors, School of Physics, Electronics and Communication, Jiangxi Normal University, Nanchang, Jiangxi 330022, China

³School of Printing and Packaging, Wuhan University, Wuhan, Hubei 430072, China

Correspondence should be addressed to Shuangli Ye; slye@whu.edu.cn

Received 27 November 2014; Accepted 31 December 2014

Academic Editor: Wen Lei

Copyright © 2015 Feng Liu et al. This is an open access article distributed under the Creative Commons Attribution License, which permits unrestricted use, distribution, and reproduction in any medium, provided the original work is properly cited.

The shell thickness-dependent strain distributions of the Au/Ag and Ag/Au core-shell nanoparticles embedded in Al₂O₃ matrix have been investigated by finite element method (FEM) calculations, respectively. The simulation results clearly indicate that there is a substantial strain applied on both the Au/Ag and Ag/Au core-shell nanoparticles by the Al₂O₃ matrix. For the Au/Ag nanoparticles, it can be found that the compressive strain existing in the shell is stronger than that on the center of core and reaches the maximum at the interface between the shell and core. In contrast, for the Ag/Au nanoparticles, the compressive strain applied on the core is much stronger than that at the interface and that in the shell. With the shell thickness increasing, both of the strains in the Au/Ag and Ag/Au nanoparticles increase as well. However, the strain gradient in the shell decreases gradually with the increasing of the shell thickness for both of Ag/Au and Au/Ag nanoparticles. These results provide an effective method to manipulate the strain distributions of the Au/Ag and Ag/Au nanoparticles by tuning the thickness of the shell, which can further have significant influences on the microstructures and physical properties of Au/Ag and Ag/Au nanoparticles.

1. Introduction

Nanoparticles with core-shell structure have attracted intensive scientific and technical interests due to their potential applications in catalysis, drug delivery, microelectronics, sensor, and many other emerging nanotechnologies [1–5]. Particularly, the bimetallic nanoparticles with core-shell structure have constantly been the subject of these studies because of their improved electronic, optical, and catalytic performances compared with those of monometallic nanoparticles [6, 7]. Moreover, it has been demonstrated that the composition, size, shape, and surface modification of these bimetallic nanoparticles can be tailored for the targeted applications [8, 9]. Among them, Au/Ag and Ag/Au core-shell nanoparticles have currently captured exponential attention due to their unique optical and photonic properties. It has been illustrated that Au and Ag present a broad absorption band in the visible

region of the electromagnetic spectrum [10–12], which can be due to the collective oscillation of the free conduction electrons induced by an interacting electromagnetic field [13]. Moreover, Au is a suitable candidate for biomedical applications because of its excellent performances on biocompatibility, chemical stability and easy surface modification, and so forth. Therefore, the Au/Ag and Ag/Au core-shell nanoparticles with surface plasmon enhancement and high levels of sensitivity have tremendous applications for optical, chemical, and bimolecular devices. For example, the generation of detectable Fano-resonance has been demonstrated in Au/Ag core-shell structure [14], which has a great potential in the subwavelength waveguides, and low-loss metamaterials sensors [15–18].

On the other hand, strain engineering provides a general strategy to control the morphology and microstructure of the nanostructures, leading to an enhancement of their device

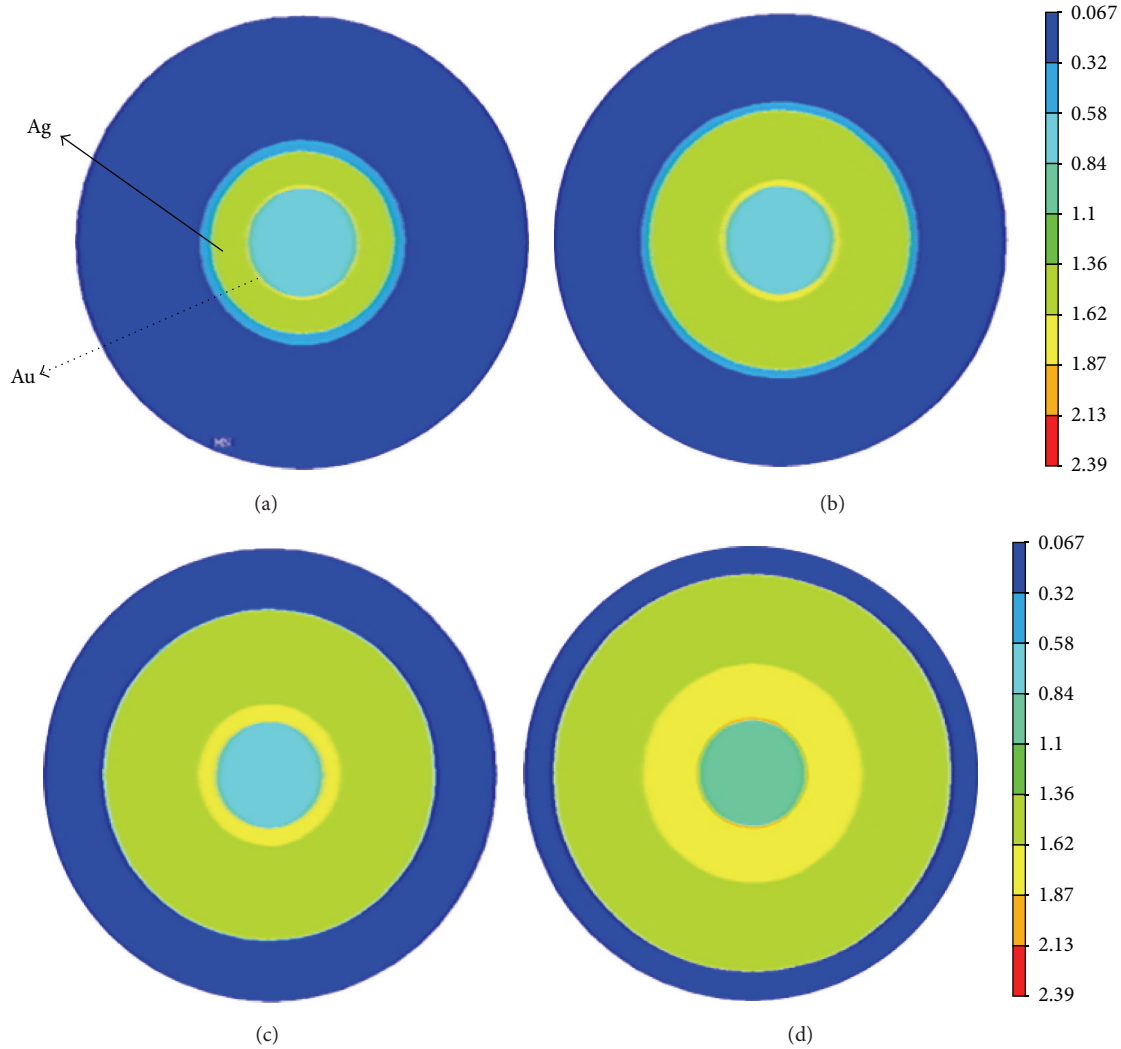


FIGURE 1: Morphological cross-sectional strain distribution of embedded core-shell Au/Ag nanoparticles with the shell thickness of (a) 2.5 nm, (b) 5 nm, (c) 7.5 nm, and (d) 10 nm, respectively.

performance. For example, quantum dots, a kind of nanostructures for making high performance nanodevices, can be realized by using self-assembled growth technique, which is based on a process of strain accumulation and relaxation in the system [19, 20]. For the core-shell nanoparticles confined in a host matrix, a substantial strain is induced [21–25], which can be used to tune the interplay between the core and shell layers, the morphology [26, 27], and optical properties [28]. Therefore, for the Au/Ag and Ag/Au core-shell nanoparticles, along with the enhanced light absorption, spectral tuning of the surface plasmon resonance by strain can provide another dimension besides the usual size and composition manipulation. Here, the shell thickness-dependent strain distributions of the Au/Ag and Ag/Au core-shell nanoparticles embedded in Al_2O_3 matrix have been investigated, respectively. The simulation results offer an effective method to manipulate the strain distributions of the Au/Ag and Ag/Au nanoparticles by tuning the thickness of the shell, which can further have significant influences on the surface states and surface plasmon resonance of Au/Ag and Ag/Au nanoparticles.

2. Methods

In this paper, a FE calculation is performed to simulate the strain distribution of embedded Au/Ag and Ag/Au core/shell nanoparticles with different shell thickness. The interplay between the strain and the structure of confined Au/Ag and Ag/Au nanoparticles has been investigated. FE calculation has been applied successfully to continuum modeling of deformation [29] of materials. Recently, simulation on the strain distribution of nanoparticles by FE method has been widely studied [30, 31]. For materials at nanoscale, the simulations by the continuum elastic FE method and the atomistic strain calculations have reached a general qualitative agreement [32, 33]. Many physical properties of nanomaterials, including elastic anisotropy, thermal expansion, and three-dimensional morphology, can be understood well by the FE simulation results. In our simulation, the FE model for the strain distribution is based upon the following assumptions. A spherical, linear-elastic core-shell Au/Ag or Ag/Au nanoparticle is confined in an isotropic and linear-elastic

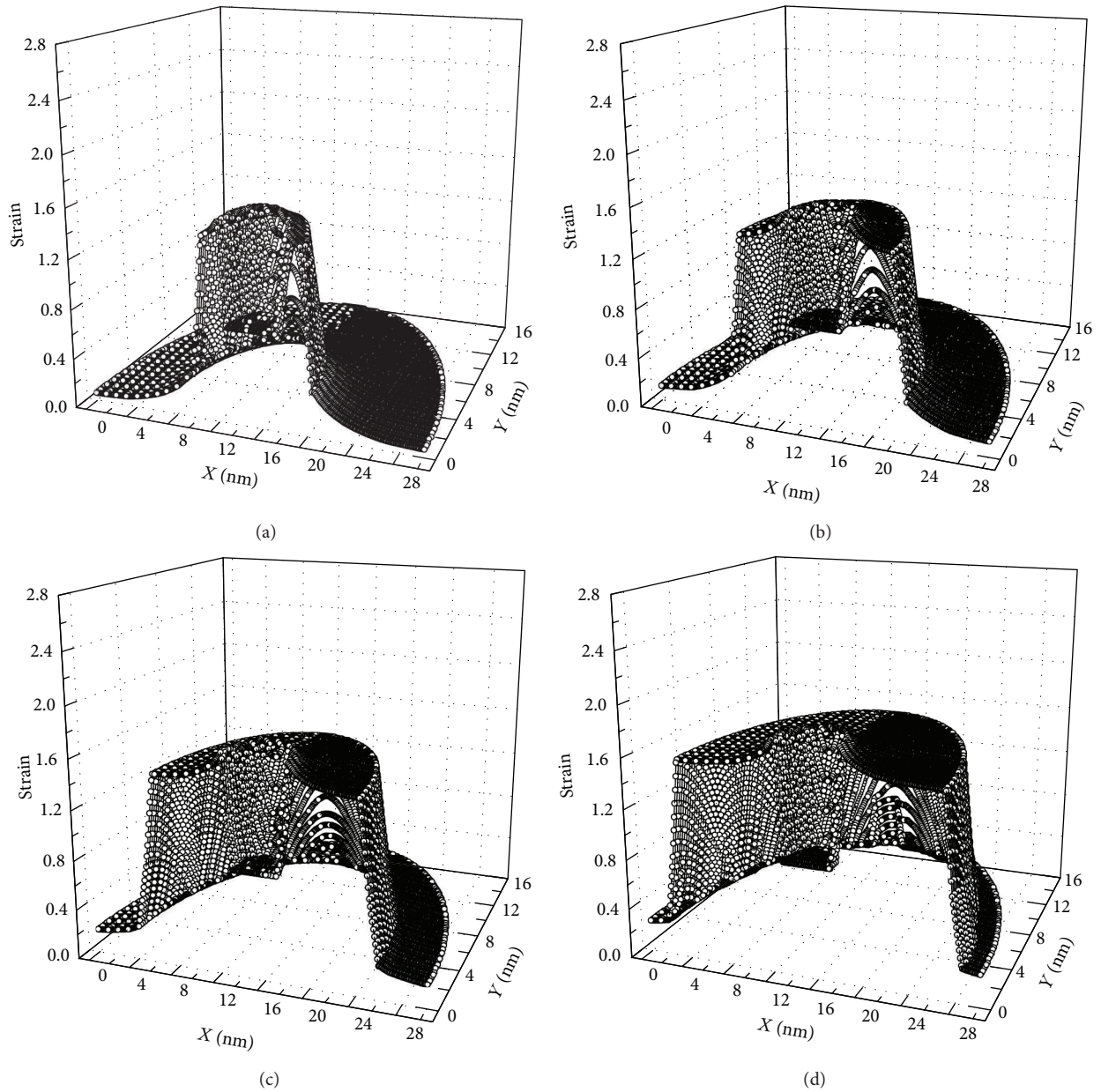


FIGURE 2: X-Y plane strain profiles for Au/Ag nanoparticles with the shell thickness of (a) 2.5 nm, (b) 5 nm, (c) 7.5 nm, and (d) 10 nm, respectively.

matrix. The Au/Ag or Ag/Au nanoparticle surface is welded to the Al_2O_3 matrix. The core size is 2.5 nm and the shell thickness is 2.5 nm, 5 nm, 7.5 nm, and 10 nm for each nanoparticle, respectively. The thermal expansion mismatch between the nanoparticles and Al_2O_3 matrix leads to a substantial strain in the confined Au/Ag or Ag/Au nanoparticles. Young's modulus is taken to be 170 GPa, 76 GPa, and 360 GPa for Au, Ag, and Al_2O_3 , while Poisson's ratio is taken to be 0.42, 0.38, and 0.24 for Au, Ag, and Al_2O_3 , respectively.

3. Results and Discussion

The morphological cross-sectional strain distributions for the core-shell Au/Ag nanoparticles embedded in Al_2O_3 thin film

with the shell thickness of 2.5 nm, 5 nm, 7.5 nm, and 10 nm are presented in Figures 1(a)–1(d), respectively. It can be found that the strain distributes inhomogeneously, which can be tuned by the shell thickness. Correspondingly, the X-Y plane strain profiles for embedded Au/Ag nanoparticle with the shell thickness of 2.5 nm, 5 nm, 7.5 nm, and 10 nm are shown in Figures 2(a)–2(d), respectively. Figures 2(a)–2(d) illustrate quantitatively that there is a large compressive strain applied on the Au/Ag nanoparticle by the Al_2O_3 matrix. The strain is weaker in the core than that in the shell. It reaches the maximum at the interface and decreases with the layer away from the interface. With the shell thickness increasing, it can be seen that the strain existing in the core-shell Au/Ag nanoparticles becomes stronger. The strain distribution in

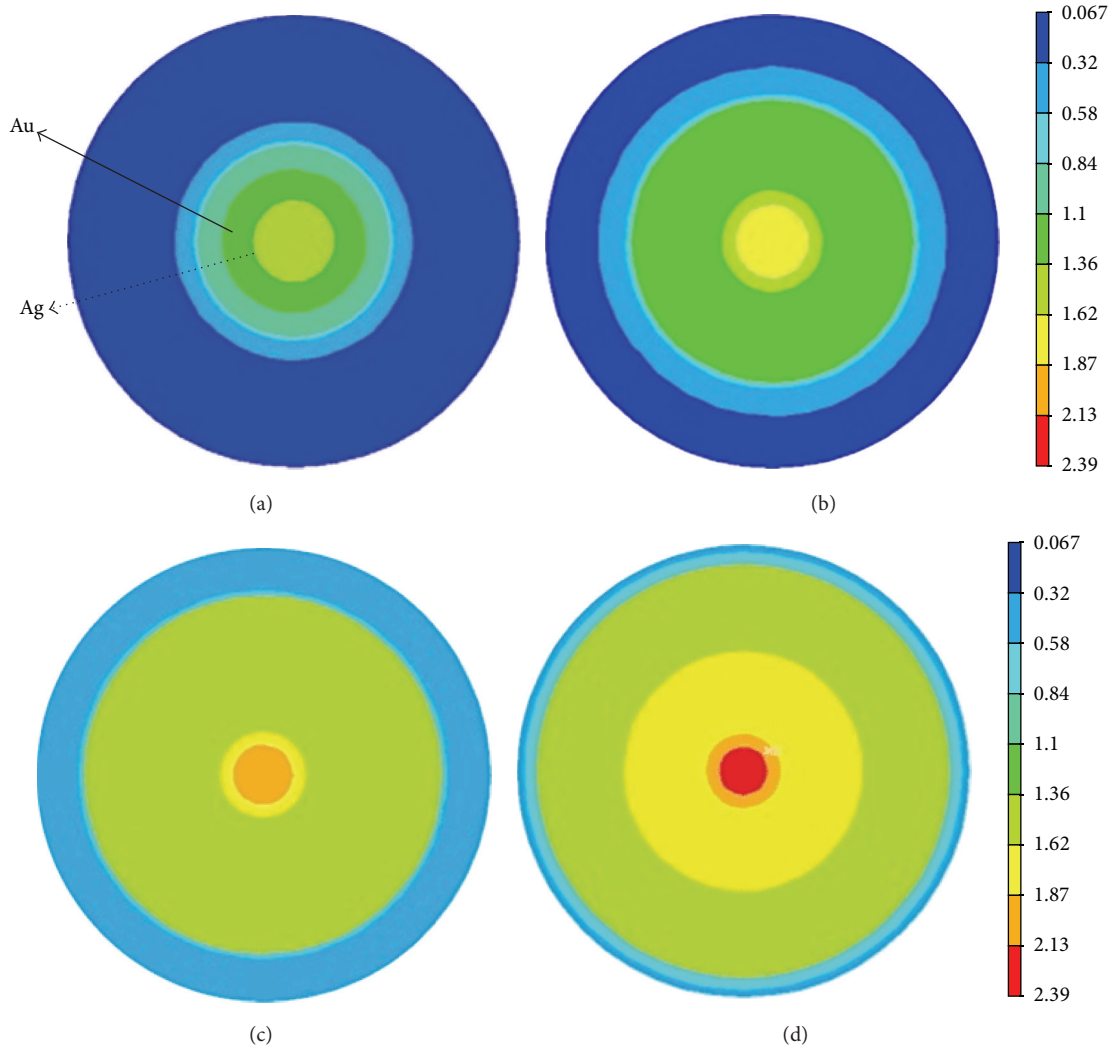


FIGURE 3: Morphological cross-sectional strain distribution of confined Ag/Au nanoparticles with the shell thickness of (a) 2.5 nm, (b) 5 nm, (c) 7.5 nm, and (d) 10 nm, respectively.

the core keeps homogenous. However, the inhomogeneity of strain distribution existing in the shell is enhanced.

Similarly, the morphological cross-sectional strain distributions for Ag/Au nanoparticles embedded in Al_2O_3 thin films with the shell thickness of 2.5 nm, 5 nm, 7.5 nm, and 10 nm are presented in Figures 3(a)–3(d), respectively. The X-Y plane strain profiles for embedded Ag/Au nanoparticle with the shell thickness of 2.5 nm, 5 nm, 7.5 nm, and 10 nm are illustrated in Figures 4(a)–4(d), respectively. It also can be seen that there is a compressive strain applied on the Ag/Au nanoparticles by the Al_2O_3 matrix. However, the strain distributes quite differently from that in the Au/Ag nanoparticle, which reaches the maximum in the core and decreases monotonously from the core to the shell in the Ag/Au nanoparticles. With the shell thickness increasing, the strain increases as well. The strain distribution in the core keeps homogenous, and the inhomogeneity of strain distribution existing in the shell is enhanced.

For a comparison, Figure 5 illustrates the strain distributions and the strain gradient for the Au/Ag and Ag/Au nanoparticles with the shell thickness of 2.5 nm, 5 nm, 7.5 nm, and 10 nm, respectively. It can be found that, for both of Au/Ag and Ag/Au nanoparticles, the strain is enhanced with the increasing of the shell thickness. Moreover, the strain increases faster for Ag/Au than that for Au/Ag nanoparticles. For these two core-shell nanoparticles with the same shell thickness, the strain on the core is larger for Ag/Au than that for Au/Ag nanoparticles, which can be due to the larger Young's modulus of Au than that of Ag. The strain gradient in the shell decreases gradually with the increasing of the shell thickness for both of Ag/Au and Au/Ag nanoparticles. However, the strain gradient in the shell decreases faster for Au/Ag than that for Ag/Au nanoparticles. The homogeneous strain distribution in the core and the inhomogeneous strain in the shell can have a significant influence on the microstructure and morphology of Au/Ag and Ag/Au nanoparticles, which

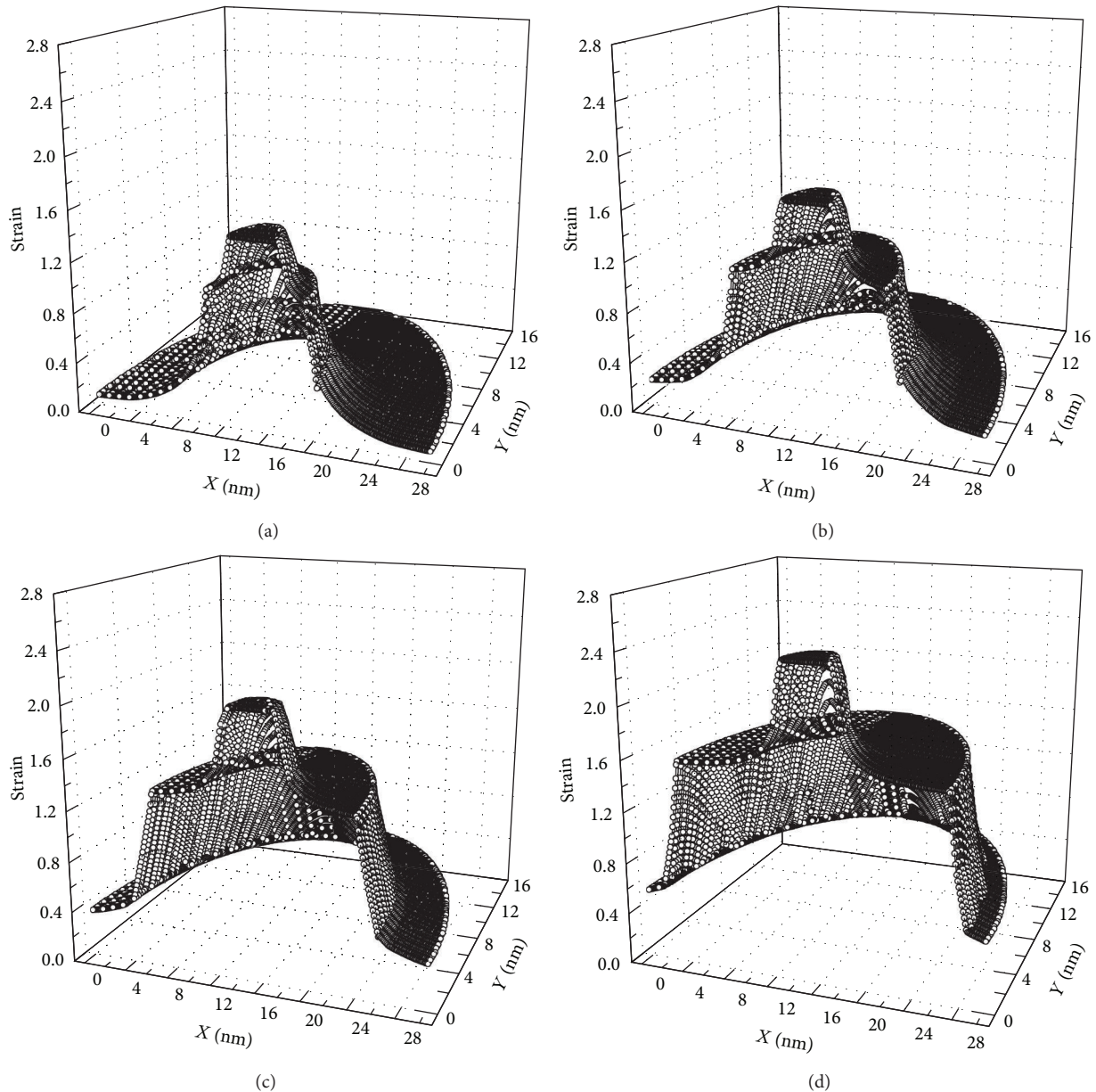


FIGURE 4: X - Y plane strain profiles of Ag/Au nanoparticles with the shell thickness of (a) 2.5 nm, (b) 5 nm, (c) 7.5 nm, and (d) 10 nm, respectively.

plays an important role in tuning the surface states and surface plasmon resonance of Au/Ag and Ag/Au nanoparticles.

4. Conclusion

In summary, the shell thickness-dependent strain distributions of the Au/Ag and Ag/Au core-shell nanoparticles embedded in Al_2O_3 matrix have been investigated by FEM calculations, respectively. The simulation results clearly indicate that there is a substantial strain applied on both the Au/Ag and Ag/Au core-shell nanoparticles by the Al_2O_3 matrix, and the strain distributes homogeneously in the core and

inhomogeneously in the shell. For the Au/Ag nanoparticle, the strain reaches the maximum at the interface and is weaker in the core than that in the shell. For the Ag/Au nanoparticles, the strain decreases monotonously from the core to the shell. For these two nanoparticles with the same shell thickness, the strain in the core is larger for Ag/Au than that for Au/Ag nanoparticles. With the shell thickness increasing, both of the strains in Au/Ag and Ag/Au nanoparticles are enhanced, and the strain gradient in the shell decreases gradually. These results demonstrate an effective method to manipulate the strain distributions of the Au/Ag and Ag/Au nanoparticles by tuning the thickness of the shell, which plays an important role in optical properties of Au/Ag and Ag/Au nanoparticles.

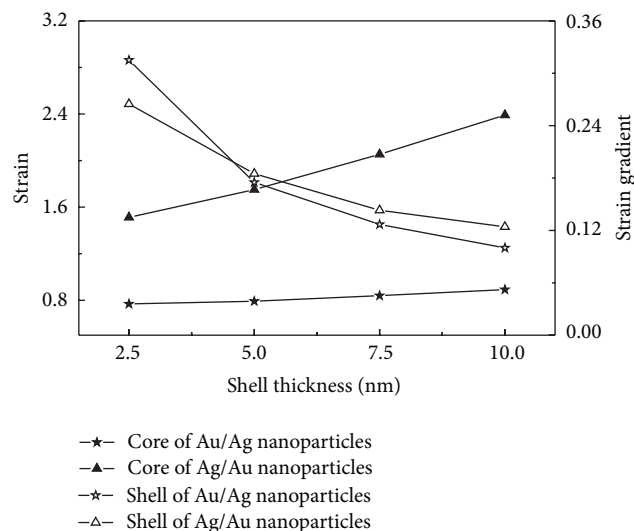


FIGURE 5: Strain on the core, strain gradient in the shell of the Au/Ag and Ag/Au nanoparticles with the shell thickness of 2.5 nm, 5 nm, 7.5 nm, and 10 nm, respectively.

Conflict of Interests

The authors declare that there is no conflict of interests regarding the publication of this paper.

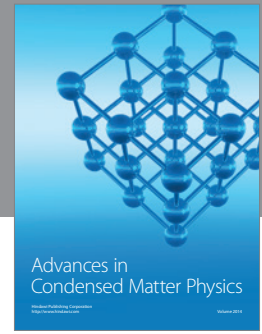
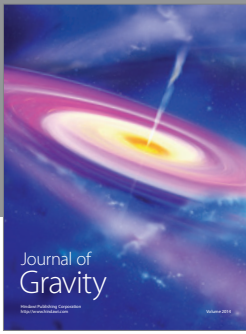
Acknowledgment

This work is supported by National Natural Science Foundation of China (Grant nos. 11164008, 51461019, 11174226, and 51371129).

References

- [1] B. Wiley, Y. Sun, and Y. Xia, "Synthesis of silver nanostructures with controlled shapes and properties," *Accounts of Chemical Research*, vol. 40, no. 10, pp. 1067–1076, 2007.
- [2] L. Lu, A. Kobayashi, K. Tawa, and Y. Ozaki, "Silver nanoplates with special shapes: controlled synthesis and their surface plasmon resonance and surface-enhanced Raman scattering properties," *Chemistry of Materials*, vol. 18, no. 20, pp. 4894–4901, 2006.
- [3] Y.-S. Shon and E. Cutler, "Aqueous synthesis of alkanethiolate-protected Ag nanoparticles using bunte salts," *Langmuir*, vol. 20, no. 16, pp. 6626–6630, 2004.
- [4] Z. S. Pillai and P. V. Kamat, "What factors control the size and shape of silver nanoparticles in the citrate ion reduction method?" *The Journal of Physical Chemistry B*, vol. 108, no. 3, pp. 945–951, 2004.
- [5] J. H. Hodak, A. Henglein, M. Giersig, and G. V. Hartland, "Laser-induced inter-diffusion in AuAg core-shell nanoparticles," *The Journal of Physical Chemistry B*, vol. 104, no. 49, pp. 11708–11718, 2000.
- [6] I. Srnová-Šloufová, F. Lednický, A. Gemperle, and J. Gemperlová, "Core-shell (Ag)Au bimetallic nanoparticles: analysis of transmission electron microscopy images," *Langmuir*, vol. 16, no. 25, pp. 9928–9935, 2000.
- [7] C. C. Li, L. Sun, Y. Q. Sun, and T. Teranishi, "One-pot controllable synthesis of au@ag heterogeneous nanorods with highly tunable plasmonic absorption," *Chemistry of Materials*, vol. 25, no. 13, pp. 2580–2590, 2013.
- [8] L. H. Lu, G. Y. Sun, H. J. Zhang et al., "Fabrication of core-shell Au-Pt nanoparticle film and its potential application as catalysis and SERS substrate," *Journal of Materials Chemistry*, vol. 14, no. 6, pp. 1005–1009, 2004.
- [9] F. Hubenthal, N. Borg, and F. Träger, "Optical properties and ultrafast electron dynamics in gold-silver alloy and core-shell nanoparticles," *Applied Physics B: Lasers and Optics*, vol. 93, no. 1, pp. 39–45, 2008.
- [10] J. Schmitt, P. Mächtle, D. Eck, H. Möhwald, and C. A. Helm, "Preparation and optical properties of colloidal gold monolayers," *Langmuir*, vol. 15, no. 9, pp. 3256–3266, 1999.
- [11] U. Kreibitz and M. Vollmer, *Optical Properties of Metal Clusters*, Springer, Berlin, Germany, 1995.
- [12] P. Mulvaney, "Surface plasmon spectroscopy of nanosized metal particles," *Langmuir*, vol. 12, no. 3, pp. 788–800, 1996.
- [13] A. K. Samal, L. Polavarapu, S. Rodal-Cedeira, L. M. Liz-Marzán, J. Pérez-Juste, and I. Pastoriza-Santos, "Size tunable Au@Ag core-shell nanoparticles: synthesis and surface-enhanced raman scattering properties," *Langmuir*, vol. 29, no. 48, pp. 15076–15082, 2013.
- [14] O. Peña-Rodríguez and U. Pal, "Au@Ag core-shell nanoparticles: efficient all-plasmonic Fano-resonance generators," *Nanoscale*, vol. 3, no. 9, pp. 3609–3612, 2011.
- [15] J. B. Lassiter, H. Sobhani, J. A. Fan et al., "Fano resonances in plasmonic nanoclusters: geometrical and chemical tunability," *Nano Letters*, vol. 10, no. 8, pp. 3184–3189, 2010.
- [16] J. A. Fan, C. Wu, K. Bao et al., "Self-assembled plasmonic nanoparticle clusters," *Science*, vol. 328, no. 5982, pp. 1135–1138, 2010.
- [17] N. Liu, T. Weiss, M. Mesch et al., "Planar metamaterial analogue of electromagnetically induced transparency for plasmonic sensing," *Nano Letters*, vol. 10, no. 4, pp. 1103–1107, 2010.
- [18] S. Mukherjee, H. Sobhani, J. B. Lassiter, R. Bardhan, P. Nordlander, and N. J. Halas, "Fanoshells: nanoparticles with built-in Fano resonances," *Nano Letters*, vol. 10, no. 7, pp. 2694–2701, 2010.
- [19] D. Gammon, "Quantum dots: strain is a problem no more," *Nature Nanotechnology*, vol. 7, no. 10, pp. 621–622, 2012.
- [20] P. J. Simmonds, C. D. Yerino, M. Sun et al., "Tuning quantum dot luminescence below the bulk band gap using tensile strain," *ACS Nano*, vol. 7, no. 6, pp. 5017–5023, 2013.
- [21] A. Wellner, V. Paillard, C. Bonafos et al., "Stress measurements of germanium nanocrystals embedded in silicon oxide," *Journal of Applied Physics*, vol. 94, no. 9, pp. 5639–5642, 2003.
- [22] A. Cheung, G. de M. Azevedo, C. J. Glover et al., "Structural perturbations within Ge nanocrystals in silica," *Applied Physics Letters*, vol. 84, no. 2, article 278, 2004.
- [23] H. G. Chew, F. Zheng, W. K. Choi, W. K. Chim, Y. L. Foo, and E. A. Fitzgerald, "Influence of reductant and germanium concentration on the growth and stress development of germanium nanocrystals in silicon oxide matrix," *Nanotechnology*, vol. 18, no. 6, Article ID 065302, 2007.
- [24] T. Benabbas, Y. Androussi, and A. Lefebvre, "A finite-element study of strain fields in vertically aligned InAs islands in GaAs," *Journal of Applied Physics*, vol. 86, no. 4, pp. 1945–1950, 1999.
- [25] Q. X. Pei, C. Lu, and Y. Y. Wang, "Effect of elastic anisotropy on the elastic fields and vertical alignment of quantum dots," *Journal of Applied Physics*, vol. 93, no. 3, pp. 1487–1492, 2003.

- [26] C. Yuan, Q. Liu, and B. Xu, "Strain-induced structural phase transition of Si nanoparticles," *The Journal of Physical Chemistry C*, vol. 115, no. 33, pp. 16374–16377, 2011.
- [27] C. L. Yuan, B. Xu, and W. Lei, "Strain-induced direct band gap LaAlO₃ nanocrystals," *Materials Letters*, vol. 68, no. 1, pp. 392–394, 2012.
- [28] C. L. Yuan, H. Cai, P. S. Lee, J. Guo, and J. He, "Tuning photoluminescence of Ge/GeO₂ core/shell nanoparticles by strain," *Journal of Physical Chemistry C*, vol. 113, no. 46, pp. 19863–19866, 2009.
- [29] H. Huebner, D. L. Dewhurst, D. E. Smith et al., *The Finite Element Method for Engineers*, John Wiley & Sons, New York, NY, USA, 2001.
- [30] C. L. Johnson, E. Snoeck, M. Ezcurdia et al., "Effects of elastic anisotropy on strain distributions in decahedral gold nanoparticles," *Nature Materials*, vol. 7, no. 2, pp. 120–124, 2008.
- [31] Z. W. Shan, G. Adesso, A. Cabot et al., "Ultrahigh stress and strain in hierarchically structured hollow nanoparticles," *Nature Materials*, vol. 7, no. 12, pp. 947–952, 2008.
- [32] J. Grönqvist, N. Søndergaard, F. Boxberg, T. Guhr, S. Åberg, and H. Q. Xu, "Strain in semiconductor core-shell nanowires," *Journal of Applied Physics*, vol. 106, no. 5, Article ID 053508, 2009.
- [33] D. Baretin, S. Madsen, B. Lassen, and M. Willatzen, "Comparison of wurtzite atomistic and piezoelectric continuum strain models: implications for the electronic band structure," *Superlattices and Microstructures*, vol. 47, no. 1, pp. 134–138, 2010.



Hindawi

Submit your manuscripts at
<http://www.hindawi.com>

